AIP Advances

Doping effect on the thermoelectric transport properties of $HfTe_5$

Cite as: AIP Advances **9**, 125021 (2019); https://doi.org/10.1063/1.5127804
Submitted: 16 September 2019 . Accepted: 30 November 2019 . Published Online: 17 December 2019

Junfeng Hu, Haiming Yu, and Jean-Philippe Ansermet

COLLECTIONS

Paper published as part of the special topic on Chemical Physics, Energy, Fluids and Plasmas, Materials Science and Mathematical Physics

View Online Export Citation CrossMark

ARTICLES YOU MAY BE INTERESTED IN

Magneto-thermoelectric characterization of a $HfTe_5$ micro-ribbon
Applied Physics Letters **115**, 072109 (2019); https://doi.org/10.1063/1.5116788

Large anomalous Nernst effect in thin films of the Weyl semimetal Co_2MnGa
Applied Physics Letters **113**, 212405 (2018); https://doi.org/10.1063/1.5048690

Experimental observation of conductive edge states in weak topological insulator candidate $HfTe_5$
APL Materials **6**, 121111 (2018); https://doi.org/10.1063/1.5050847

Call For Papers!
AIP Advances
SPECIAL TOPIC: Advances in Low Dimensional and 2D Materials

AIP Publishing

© 2019 Author(s).

Doping effect on the thermoelectric transport properties of $HfTe_5$

Cite as: AIP Advances 9, 125021 (2019); doi: 10.1063/1.5127804
Submitted: 16 September 2019 • Accepted: 30 November 2019 •
Published Online: 17 December 2019

View Online Export Citation CrossMark

Junfeng Hu,[1,2] Haiming Yu,[1,a)] and Jean-Philippe Ansermet[2,b)]

AFFILIATIONS

[1] Fert Beijing Institute, BDBC, School of Microelectronics, Beihang University, Xueyuan Road 37, Beijing 100191, China
[2] Institute of Physics, Station 3, Ecole Polytechnique Fédérale de Lausanne, 1015 Lausanne, Switzerland

[a)] Electronic mail: haiming.yu@buaa.edu.cn
[b)] Electronic mail: jean-philippe.ansermet@epfl.ch

ABSTRACT

We studied the influence of doping $HfTe_5$ with 5% Ti on electric (resistivity and the Hall effect) and thermoelectric transport properties (the Seebeck coefficient, magneto-thermoelectric power, and Nernst effect). The properties of 5% Ti-doped $HfTe_5$ do not change much. Nernst coefficients larger than magneto-thermoelectric power were observed in a temperature range near the compensation temperature at which the Seebeck coefficient vanishes. This indicates that a two-carrier conduction model could describe our experimental results. Owing to the high thermoelectric performance, thermopiles were made on a printed circuit board based on doped and undoped $HfTe_5$. A large Seebeck voltage was obtained at room temperature. It became even larger in a low temperature range and presented strong magnetic field dependence.

© 2019 Author(s). All article content, except where otherwise noted, is licensed under a Creative Commons Attribution (CC BY) license (http://creativecommons.org/licenses/by/4.0/). https://doi.org/10.1063/1.5127804

I. INTRODUCTION

In recent years, the issue of energy has received more and more attention particularly because of the ubiquity of information technology. Energy consumption and heat dissipation in integrated circuits are some of the problems. To find suitable materials that can efficiently use wasted heat for power generation is a hot topic in thermoelectricity.[1] Due to materials nanoscience and nanofabrication technology, low-dimensional thermoelectric materials open a new direction for thermoelectricity research.[2,3] For example, Linden *et al.*[4] have recently proposed the use of fabric-based thermopiles as thermoelectric generators that can take advantage of the heat of the human body to power wearable electronic devices.[5] Efforts have been made for the optimization of thermoelectric power generators in many ways, such as the geometry structure of the thermopiles,[6] polymer gels with a tunable ionic Seebeck coefficient,[7] and the reduction of a heat source or sink thermal resistances for high performance thermoelectric coolers.[8] Alternative thermoelectric devices have also been proposed.[9,10] In particular, topological quantum materials have begun to attract growing attention because the novel electronic structure of topological insulators opens new opportunities for thermoelectric materials with high performance.[11,12] The large thermopower of these materials shows their potential to be used as thermoelectric applications. In these materials, applying an external magnetic field can further enhance high-thermoelectric performance.[13–15]

In parallel to these efforts in thermoelectric power generation, the field of spin caloritronics,[16,17] which studies the interaction between spin, charge, and heat currents, has further stimulated fundamental interest in thermoelectricity, most notably, the spin Seebeck effect.[18–20] Thermopiles based on the anomalous Nernst effect (ANE) provide another possibility for new thermoelectric applications due to their three-dimensional nature as it can be used with the heat source in any direction.[21–25] Materials with large thermoelectric effects and strong magnetic field-dependent behaviors may offer useful options. Layered hafnium pentatelluride ($HfTe_5$) and $ZrTe_5$ single crystals, its cousin material, have stimulated several experimental studies.[26,27] Here, we report on simple thermopiles based on $HfTe_5$, a material which has been studied for a long time[28–30] and recently regained attention due to its possible topological properties.[31] We considered $HfTe_5$ with 5% Ti doping in the hope of finding ways to further improve thermoelectric performance.[32,33]

© Author(s) 2019

II. METHODS

Ribbonlike single crystals of undoped $HfTe_5$ and doped $Hf_{0.95}Ti_{0.05}Te_5$ were grown in similar conditions as reported previously.[28,34] The typical size of $HfTe_5$ and $Hf_{0.95}Ti_{0.05}Te_5$ single crystals used for thermoelectric measurements were about 10 mm in length, 1 mm in width, and 0.2–0.3 mm in thickness. We used smaller crystals for the electrical transport measurements. All the samples presented slight differences, but the key features were basically the same. All thermoelectric measurements were performed on a homebuilt setup, and the electric transport measurements were performed on a Quantum Design Physical Property Measurement System (PPMS). More details can be found in the supplementary material of a previous paper.[15]

III. RESULTS AND DISCUSSION

We first characterized the electric transport properties (resistivity, magnetoresistance, and the Hall effect) in $Hf_{0.95}Ti_{0.05}Te_5$ (sample 1), as shown in Fig. 1. All the magnetic field-dependent measurements were performed at temperatures below 160 K, at which the magnetic field starts to influence the transport properties [Figs. 1(a)–1(b)]. Large magnetoresistivity [Fig. 1(c)] was observed with strong dependence on temperature when the external magnetic field was applied out-of-plane. The results of the Hall effect show a sign reversal of the Hall coefficients [Fig. 1(d)]. All these results are consistent with those obtained with $HfTe_5$,[15] which means 5% Ti doping does not significantly change the sample properties. A two-carrier model could be used to explain these experimental results.[15,35–37] The electron (hole) concentration [Fig. 1(e)] and mobility [Fig. 1(f)] are extracted from the Hall resistivity by using the following equation,[38] which indicates a possible transition as the temperature changed from 110 K to 30 K:

$$\rho_{xy}(B) = \frac{\rho_e^2 R_h + \rho_h^2 R_e + R_h R_e (R_h + R_e) B^2}{(\rho_h + \rho_e)^2 + (R_h + R_e)^2 B^2} B, \quad (1)$$

where $\rho_e = \frac{1}{n_e e \mu_e}$ and $\rho_h = \frac{1}{n_h e \mu_h}$ are electron and hole resistivities, respectively, n_e and n_h are the carrier concentrations for electron-like (EL) and hole-like (HL) bands, and μ_e and μ_h are the carrier mobilities for electron-like (EL) and hole-like (HL) bands. $R_e = \frac{-1}{n_e e}$ and $R_h = \frac{1}{n_h e}$ are Hall coefficients for the electron and hole, respectively, with an elementary charge e ($\approx 1.6 \times 10^{-19}$ C).

The temperature-dependent resistivity of both $HfTe_5$ and $Hf_{0.95}Ti_{0.05}Te_5$ (sample 2) at zero magnetic field is normalized with a resistivity of 300 K [Fig. 2(a)]. The resistivity for both samples decreases at first and then increases sharply to a maximum, at around the transition temperature T_p. Beyond that, the resistivity drops rapidly as the temperature is further decreased. The reason why 5% Ti doped $Hf_{0.95}Ti_{0.05}Te_5$ has lower T_p is probably because the Ti atoms are smaller than the Hf atoms and this should result in some slight lattice compression, which can be assimilated to an external pressure.[29] Strong influence of the out-of-plane magnetic field ($B \parallel b$) is observed, namely, a large increase in resistivity in the low temperature range and a shift of T_p to a higher temperature. This was observed in both types of samples [see inset Fig. 2(a)]. Similar temperature-dependent behaviors for thermopower can be seen in Fig. 2(b) at zero magnetic field, except for the additional peak in $HfTe_5$ around 100 K. In general, the Seebeck coefficients S for both crystals increase slightly when the temperature is decreased around the transition temperature T_p, which are 70 K and 58 K for $HfTe_5$ and $Hf_{0.95}Ti_{0.05}Te_5$, respectively. This temperature is slightly different from the one obtained with the sample used for resistivity measurements. At lower temperatures, the Seebeck coefficient goes through a minimum. The sign change of S, which can be attributed to a change of the majority charge carrier from HL to EL carriers, was first observed in the pioneering work of Jones *et al.*[28]

Consistent with sample 1, large magnetoresistance [Fig. 3(a)] and the Hall effect [Fig. 3(b)] were observed in sample 2 as well. Moreover, the magneto-thermoelectric power and Nernst effect have been measured in $Hf_{0.95}Ti_{0.05}Te_5$ [sample 3, Figs. 3(c) and 3(d)]. Corresponding measurements for $HfTe_5$ can be found in the studies by Hu *et al.*[15] The thermopower and Nernst effects measured at different temperatures as a function of magnetic field applied along the b axis in $Hf_{0.95}Ti_{0.05}Te_5$ are shown in Figs. 3(c) and 3(d), respectively. As already shown in Fig. 2(b), the temperature greatly affects the thermopower even at zero magnetic field. Here, a large influence of the external magnetic field has been observed at a fixed temperature. For example, at 47 K, the thermopower changes from around −70 μV/K at zero magnetic field to as much as −229 μV/K at a

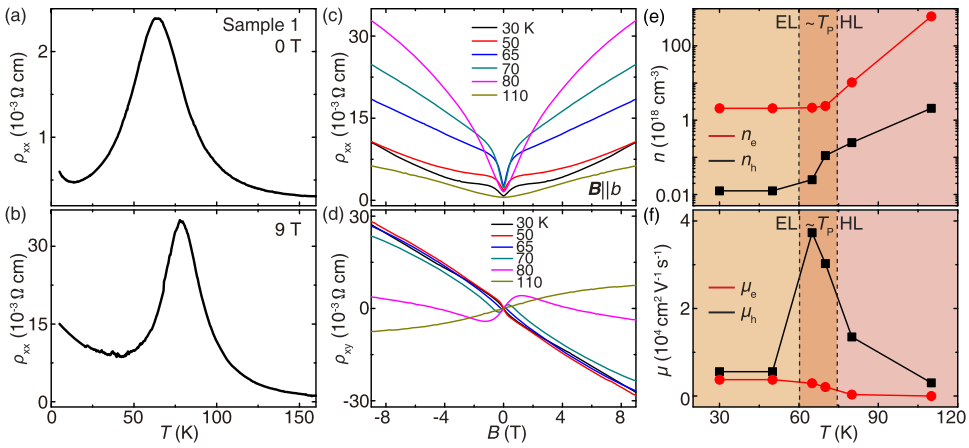

FIG. 1. Electric transport measurements of $Hf_{0.95}Ti_{0.05}Te_5$ on sample 1 ($3 * 0.83 * 0.094$ mm^3): (a) temperature-dependent resistivity at zero magnetic field, (b) temperature-dependent resistivity at 9 T, (c) magnetic field-dependent magnetoresistivity measured at variable temperatures, and (d) the dependence of Hall resistivity on magnetic field measured at variable temperatures from 30 K to 110 K; (e) and (f) are the electron (hole) concentration and mobility, respectively. Data were obtained with sample 1.

© Author(s) 2019

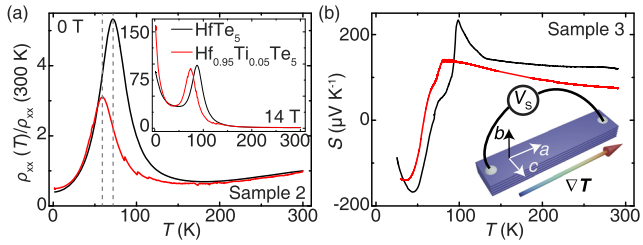

FIG. 2. Temperature-dependent resistivity ratio and Seebeck coefficient of $HfTe_5$ and $Hf_{0.95}Ti_{0.05}Te_5$: (a) resistivity as a function of temperature normalized with the resistivity of 300 K; inset: resistivity measured with a 14 T magnetic field applied along the b axis and (b) the temperature-dependent Seebeck coefficient; inset: measurement configuration. The data of $Hf_{0.95}Ti_{0.05}Te_5$ (red curve) were obtained with samples 2 and 3. The data of $HfTe_5$ (black curve) were obtained from the studies by Hu *et al.*[15]

relatively small magnetic field of 0.35 T. The Nernst effect, which was measured with a magnetic field in the *b* direction and a temperature gradient in the *a* direction, can be simply considered as a transverse thermopower, i.e., measured in the *c* direction like the Hall effect. Around the transition temperature T_p (58 K), a large Nernst coefficient of 215 μV/K was obtained at a magnetic field of only 0.2 T. The Nernst coefficient becomes even larger at a slightly higher temperature but drops dramatically at much higher or lower temperatures, with the sign changing as shown in Fig. 3(d).

A two-carrier model for thermoelectric transport properties (the Seebeck and Nernst coefficients as a function of magnetic field) has also been proposed by Putely.[38] One essential feature that a model must account for is the step-like field dependence on the Nernst effect which resembles the ANE of ferromagnetic thin films.[25] Since the $Hf_{0.95}Ti_{0.05}Te_5$ is not a magnetic material, the anomalous behavior is presumably from an internal effective magnetic field. We can expect the Berry curvature to play a role since it has been suggested that $HfTe_5$ may have Dirac semimetal properties.[15,27] As a consequence, we cannot account for the main features of the Hall resistivity at low temperatures (below 65 K).

In view of the high thermoelectric performance of $HfTe_5$ and $Hf_{0.95}Ti_{0.05}Te_5$, we designed a simple thermopile with nine $HfTe_5$ ($Hf_{0.95}Ti_{0.05}Te_5$) stripes connected with copper wires on a printed circuit board (PCB) about 1 × 1 cm^2 in size [Fig. 4(a)]. We first measured at room temperature the output thermoelectric voltages as a function of the temperature difference applied between the two rows of copper contacts [Fig. 4(a)]. The temperature difference was measured by two Pt100 on each side of the thermopile. For a temperature difference of 40 K, a large voltage of more than 30 mV could be measured for both materials. The temperature-dependent thermopower of the thermopiles is shown in Fig. 4(b). A large thermopower, more than 1 mV/K, is obtained at low temperature. The transition temperature T_p differs for both $HfTe_5$ and $Hf_{0.95}Ti_{0.05}Te_5$ compared to the results we obtained with a single needle. This is probably caused by the difference in the qualities of crystals that are used when making a thermopile.

We also measured the magnetic field-dependent thermopower of these devices in the low temperature range where the magnetic field influences the thermopower a lot. Figs. 4(c) and 4(d) show the results for $HfTe_5$ and $Hf_{0.95}Ti_{0.05}Te_5$, respectively. The temperatures marked in the figures are the average temperatures for the cold and hot sides. By using a heater on the hot side, a very large temperature difference was generated. The temperature difference was changed at different sample temperatures. A very large output voltage of more than 0.1 V was obtained in both devices, with strong magnetic field dependence. For example, the thermoelectric voltage at 118 K changes from around 110 mV at zero magnetic field to as much as 120 mV (here, the cold side was 68 K, while the hot side

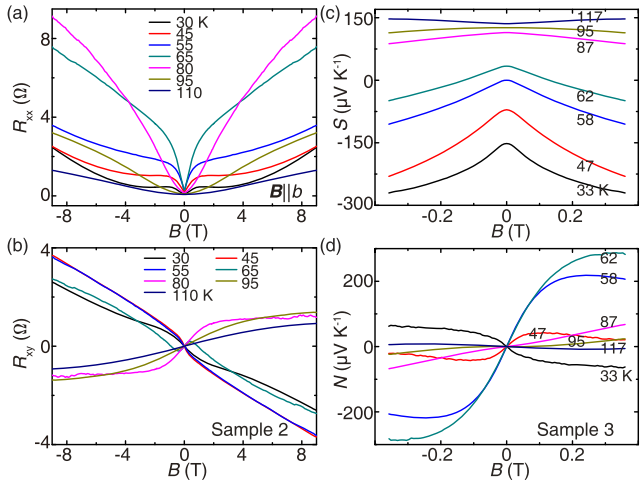

FIG. 3. Magnetic field-dependent electric and thermoelectric transport measurements of $Hf_{0.95}Ti_{0.05}Te_5$ at different temperatures below 150 K: (a) and (b) are magnetoresistance and Hall resistance and (c) and (d) are the magneto-thermoelectric power and Nernst coefficients. The magnetic field was applied in the out-of-plane direction in all measurements. Data were obtained with samples 2 and 3.

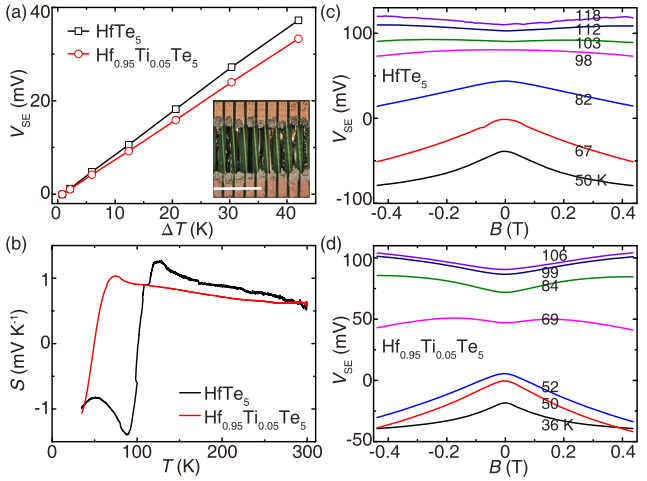

FIG. 4. Thermopiles for thermoelectric power generation: (a) thermoelectric voltage obtained from the thermopiles at room temperature; inset: the optical image of the real thermopile device; the scale bar is 5 mm, (b) the Seebeck coefficient of the thermopiles as a function of temperature, and (c) and (d) are the magneto-thermoelectric voltages measured on the thermopiles at lower temperatures for $HfTe_5$ and $Hf_{0.95}Ti_{0.05}Te_5$, respectively.

© Author(s) 2019

was 168 K; hence, the temperature difference was about 100 K) with only a 0.4 T external magnetic field applied on $HfTe_5$. A similar large change of about 40 mV is observed in $Hf_{0.95}Ti_{0.05}Te_5$ at 50 K, which is also close to the transition temperature T_p.

IV. CONCLUSIONS

In conclusion, we performed both electric and thermoelectric transport measurements on 5% Ti doped $Hf_{0.95}Ti_{0.05}Te_5$ single crystals. Compared with the undoped $HfTe_5$, the minimal doping we considered does not change the main properties of this material, except shifting the transition temperature T_p. However, high thermoelectric performance could be expected from a more detailed investigation of different Ti concentrations or different material doping in this system.[39,40] Simple thermopiles were designed and tested by using printed-board technology to form a series of 9 thermocouples composed of crystals and copper wires. A large output voltage was obtained at room temperature that could be further enhanced by lowering the temperature and applying a small external magnetic field. In view of the rapid developments that can happen in materials nanoscience and nanofabrication technology, $HfTe_5$ thin film-based thermopiles might become a promising candidate for thermoelectric power generation and in magnetic sensors.

ACKNOWLEDGMENTS

We wish to acknowledge the support from the National Natural Science Foundation of China under Grant Nos. 11674020 and U1801661, the Sino-Swiss Science and Technology Cooperation (SSSTC, Grant No. EG 01-122016) for J.H., the Program of Introducing Talents of Discipline to Universities in China, "111 Program," Grant No. B16001, and the National Key Research and Development Program of China (Grant No. 254).

REFERENCES

[1] T. Zhu, Y. Liu, C. Fu, J. P. Heremans, J. G. Snyder, and X. Zhao, Adv. Mater. **29**, 1605884 (2017).
[2] M. S. Dresselhaus, G. Chen, M. Y. Tang, R. G. Yang, H. Lee, D. Z. Wang, Z. F. Ren, J.-P. Fleurial, and P. Gogna, Adv. Mater. **19**, 1043–1053 (2007).
[3] J. P. Heremans, M. S. Dresselhaus, L. E. Bell, and D. T. Morelli, Nat. Nanotechnol. **8**, 471–473 (2013).
[4] L. K. Allison and T. L. Andrew, Adv. Mater. Technol. **4**, 1800615 (2019).
[5] D. Bradley, Mater. Today **24**, 7–8 (2019).
[6] K. V. Selvan and M. S. M. Ali, IEEE Trans. Electron Dev. **65**, 3394–3400 (2018).
[7] D. Zhao, A. Martinelli, A. Willfahrt, T. Fischer, D. Bernin, Z. U. Khan, M. Shahi, J. Brill, M. P. Jonsson, S. Fabiano, and X. Crispin, Nat. Commun. **10**, 1093 (2019).
[8] R. A. Kishore, A. Nozariasbmarz, B. Poudel, M. Sanghadasa, and S. Priya, Nat. Commun. **10**, 1765 (2019).
[9] M.-H. Liao and M. S. M. Ali, AIP Adv. **8**, 015020 (2018).
[10] K. Nan, S. D. Kang, K. Li, K. J. Yu, F. Zhu, J. Wang, A. C. Dunn, C. Zhou, Z. Xie, M. T. Agne, H. Wang, H. Luan, Y. Zhang, Y. Huang, G. Jeffrey Snyder, and J. A. Rogers, Sci. Adv. **4**, eaau5849 (2018).
[11] L. Müchler, F. Casper, B. Yan, S. Chadov, and C. Felser, Phys. Status Solidi RRL **7**, 91–100 (2012).
[12] J. P. Heremans, R. J. Cava, and N. Samarth, Nat. Rev. Mater. **2**, 17049 (2017).
[13] H. Wang, X. Luo, W. Chen, N. Wang, B. Lei, F. Meng, C. Shang, L. Ma, T. Wu, X. Dai, Z. Wang, and X. Chen, Sci. Bull. **63**, 411–418 (2018).
[14] S. J. Watzman, T. M. McCormick, C. Shekhar, S.-C. Wu, Y. Sun, A. Prakash, C. Felser, N. Trivedi, and J. P. Heremans, Phys. Rev. B **97**, 161404(R) (2018).
[15] J. Hu, M. Caputo, E. B. Guedes, S. Tu, E. Martino, A. Magrez, H. Berger, J. H. Dil, H. Yu, and J.-P. Ansermet, Phys. Rev. B **100**, 115201 (2019).
[16] H. Yu, S. D. Brechet, and J.-P. Ansermet, Phys. Lett. A **381**, 825–837 (2017).
[17] J.-P. Ansermet and S. D. Brechet, Entropy **20**, 912 (2018).
[18] K. Uchida, M. Ishida, T. Kikkawa, A. Kirihara, T. Murakami, and E. Saitoh, J. Phys.: Condens. Matter **26**, 343202 (2014).
[19] A. Kirihara, K. Kondo, M. Ishida, K. Ihara, Y. Iwasaki, H. Someya, A. Matsuba, K.-i. Uchida, E. Saitoh, N. Yamamoto, S. Kohmoto, and T. Murakami, Sci. Rep. **6**, 23114 (2016).
[20] K. Uchida, H. Adachi, T. Kikkawa, A. Kirihara, M. Ishida, S. Yorozu, S. Maekawa, and E. Saitoh, Proc. IEEE **104**, 1946–1973 (2016).
[21] Y. Sakuraba, K. Hasegawa, M. Mizuguchi, T. Kubota, S. Mizukami, T. Miyazaki, and K. Takanashi, Appl. Phys. Express **6**, 033003 (2013).
[22] Y. Sakuraba, Scr. Mater. **111**, 29–32 (2016).
[23] D.-J. Kim, K.-D. Lee, S. Surabhi, S.-G. Yoon, J.-R. Jeong, and B.-G. Park, Adv. Funct. Mater. **26**, 5507–5514 (2016).
[24] M. Ikhlas, T. Tomita, T. Koretsune, M.-T. Suzuki, D. Nishio-Hamane, R. Arita, Y. Otani, and S. Nakatsuji, Nat. Phys. **13**, 1085–1090 (2017).
[25] J. Hu, B. Ernst, S. Tu, M. Kuveždić, A. Hamzić, E. Tafra, M. Basletić, Y. Zhang, A. Markou, C. Felser, A. Fert, W. Zhao, J.-P. Ansermet, and H. Yu, Phys. Rev. Appl. **10**, 044037 (2018).
[26] J. Niu, J. Wang, Z. He, C. Zhang, X. Li, T. Cai, X. Ma, S. Jia, D. Yu, and X. Wu, Phys. Rev. B **95**, 035420 (2017).
[27] A. C. Niemann, J. Gooth, Y. Sun, F. Thiel, A. Thomas, C. Shekhar, V. Süß, C. Felser, and K. Nielsch, Appl. Phys. Lett. **115**, 072109 (2019).
[28] T. E. Jones, W. W. Fuller, T. J. Wieting, and F. Levy, Solid State Commun. **42**, 793–798 (1982).
[29] R. T. Littleton, T. M. Tritt, C. R. Feger, J. Kolis, M. L. Wilson, M. Marone, J. Payne, D. Verebeli, and F. Levy, Appl. Phys. Lett. **72**, 2056 (1998).
[30] Y.-Y. Lv, X. Li, L. Cao, D. Lin, S.-H. Yao, S.-S. Chen, S.-T. Dong, J. Zhou, Y. B. Chen, and Y.-F. Chen, Phys. Rev. Appl. **9**, 054049 (2018).
[31] H. M. Weng, X. Dai, and Z. Fang, Phys. Rev. X **4**, 011002 (2014).
[32] V. Jovovic and J. P. Heremans, J. Electron. Mater. **38**, 1504 (2009).
[33] M. D. Nielsen, C. M. Jaworski, and J. P. Heremans, AIP Adv. **5**, 053602 (2015).
[34] F. Lévy and H. Berger, J. Cryst. Growth **61**, 61–68 (1983).
[35] S.-S. Chen, X. Li, Y.-Y. Lv, L. Cao, D. lin, S.-H. Yao, J. Zhou, and Y. B. Chen, J. Alloy. Compd. **764**, 540–544 (2018).
[36] B. Fauqué, X. Yang, W. Tabis, M. Shen, Z. Zhu, C. Proust, Y. Fuseya, and K. Behnia, Phys. Rev. Mater. **2**, 114201 (2018).
[37] B. He, Y. Wang, M. Q. Arguilla, N. D. Cultrara, M. R. Scudder, J. E. Goldberger, W. Windl, and J. P. Heremans, Nat. Mater. **18**, 568–572 (2019).
[38] E. H. Putley, *The Hall Effect and Semiconductor Physics* (Dover, New York, 1968).
[39] Y. Pei, H. Wang, and G. J. Snyder, Adv. Mater. **24**, 6125–6135 (2012).
[40] N. D. Lowhorn, T. M. Tritt, E. E. Abbott, and J. W. Kolis, Appl. Phys. Lett. **88**, 022101 (2006).

© Author(s) 2019